Noise in detection of qubit states using a quantum point contact

Neil Oxtoby[a], He-Bi Sun[a]and Howard M. Wiseman[b]

[a]Centre for Quantum Computer Technology, Department of Physics, University of Queensland, St. Lucia, QLD 4072, Australia
[b]Centre for Quantum Computer Technology, School of Science, Griffith University, Nathan, QLD 4111 Australia

ABSTRACT

We present a model for detection of the states of a coupled quantum dots (qubit) by a quantum point contact. Most proposals for measurements of states of quantum systems are idealized. However in a real laboratory the measurements cannot be perfect due to practical devices and circuits. The models using ideal devices are not sufficient for describing the detection information of the states of the quantum systems. Our model therefore includes the extension to a non-ideal measurement device case using an equivalent circuit. We derive a quantum trajectory that describes the stochastic evolution of the state of the system of the qubit and the measuring device. We calculate the noise power spectrum of tunnelling events in an ideal and a non-ideal quantum point contact measurement respectively. We found that, for the strong coupling case it is difficult to obtain information of the quantum processes in the qubit by measurements using a non-ideal quantum point contact. The noise spectra can also be used to estimate the limits of applicability of the ideal model.

Keywords: qubit, quantum point contact, quantum master equation, noise spectrum, quantum trajectory

1. INTRODUCTION

Many theories for the measurement of the states of quantum systems, such as quantum dots, are idealized.[1–3] That is, the uncertainty in the conditioned state of the quantum system is due purely to the stochastic nature of the quantum processes. Such a perfect measurement is not possible in a real laboratory due to practical devices and circuitry. It is desirable to have a realistic model of this kind of measurement so that realistically available results can be related to the state of the quantum system. There have been a number of recent suggestions for (solid state) quantum computer architecture involving quantum dots of varying kinds.[4–6] A knowledge of how to read out physical properties, such as charge, at a single-electron level is required for these proposals to be practical.[1] Various devices have been proposed to measure coupled-dot systems. In particular, quantum point contacts (QPCs)[7,8] and single electron transistors (SETs).[1,2,9]

We consider continuous measurement of the state of a pair of coupled quantum dots by a non-ideal QPC. The dots are occupied by a single electron that can tunnel coherently between them, thus allowing the pair to be considered as a qubit.

The system and its functionality are detailed in Sect. 2. In Sect. 3 we model the quantum measurement of the qubit state. We derive a quantum trajectory that describes the stochastic evolution of the state of the system of the qubit and the measuring device. The calculated results as noise power spectra for the measurements of qubit states with an ideal and non-ideal QPC are presented in Sect. 4. The influence of the non-ideal components on the noise spectrum is analyzed by comparing with the spectra of the ideal QPC case. Finally, we discuss and summarize in Sect. 5. We found that, for the strong coupling (between two dots) case it is difficult to obtain information of the quantum processes in the qubit by measurements using a non-ideal quantum point contact. The limits of applicability of the ideal model can also be estimated from the noise power spectra.

Further author information: (Send correspondence to H.-B. Sun)
H.-B. Sun.: E-mail: sun@physics.uq.edu.au, Telephone: 61 7 3365 2816
H.M. Wiseman: E-mail: H.Wiseman@griffith.edu.au, Telephone: 61 7 3875 7271

Noise and Information in Nanoelectronics, Sensors, and Standards, L. B. Kish, F. Green, G. Iannaccone, J. R. Vig, Editors, Proceedings of SPIE Vol. 5115 (2003) © 2003 SPIE · 0277-786X/03/$15.00

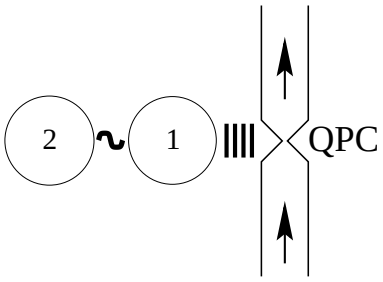

Figure 1. Schematic representation of the measurement of two coupled quantum dots occupied by a single electron using a QPC.

2. THE SYSTEM

The schematic diagram is depicted in Fig. 1. The quantum system to be measured is a pair of spatially separated and coherently coupled dots occupied by a single electron. Dot 1 is located near the QPC and is called the target. Each dot is assumed to have only one available state. The interaction between the target and the QPC is via a Coulomb blockade. The state of the qubit (the coupled dots) at a particular time is determined by the location of the electron at that time. The electron tunnelling rate through the QPC is influenced by the location of the qubit electron in a similar way that the gate voltage controls the tunnelling rate in general cases. We assume that when the electron is located in dot 2 the tunnelling rate is denoted by λ_0 and an additional tunnelling rate of λ_1 (> 0) occurs when dot 1 is occupied. The quantum point contact (QPC) is therefore used as a detector to measure the state of the qubit. In the perfect case λ_0 is zero however Johnson noise gives nonzero quiescent tunnelling rate.

For measurement of the qubit states by a non-ideal QPC, the current measured by an observer involves more than just the tunnelling events through the QPC. A real measurement circuit involves a number of noise sources from circuit components as well as the quantum noise due to the stochastic nature of the tunnelling processes through the QPC. We construct an equivalent circuit and analyze it to obtain an expression for the measured current at time t, I(t), which will be detailed in Sect. 3. Figure 2 shows the equivalent circuit we use to model our measurement of the qubit states using a non-ideal QPC. The circuit consists of the QPC, a current amplifier and miscellaneous circuit components. We model the QPC tunnel junction as a capacitance, C_1, in parallel with a *parasitic* capacitance, C_P, that exists between the source and drain 2DEGs. Typically, due to the larger 'area' of C_P, $C_P \gg C_1$. In the analysis, we consider the equivalent parallel capacitance $C = C_1 + C_P$. We refer to C as the equivalent capacitor. Tunnelling events through the QPC are modelled as a current source. The circuit has an equivalent resistance R. We have a non-ideal, DC bias voltage consisting of an ideal voltage, ε, in series with an input noise voltage source e_{In}. The Johnson noise of R is included in e_{In}. The measured current, I, is measured with an ideal ammeter after amplification by a non-ideal current amplifier. This introduces an output noise into the measured current, e_{Out}/R'. The current amplifier is at the laboratory temperature T'. These circuit components introduce an input noise into the current through the QPC.

3. FORMALISM

3.1. Ideal QPC case

The total Hamiltonian of the qubit dots is

$$H = \hbar \sum_{j=1}^{2} \omega_j c_j^\dagger c_j + i\hbar \frac{\Omega}{2}(c_1^\dagger c_2 - c_2^\dagger c_1) \tag{1}$$

where Ω is the coupling frequency and c_j and $c_j^\dagger$ ($j = 1, 2$) are the Fermi annihilation and creation operators for the single electron states within the qubit quantum dots. The second term of the right hand side of equation (1)

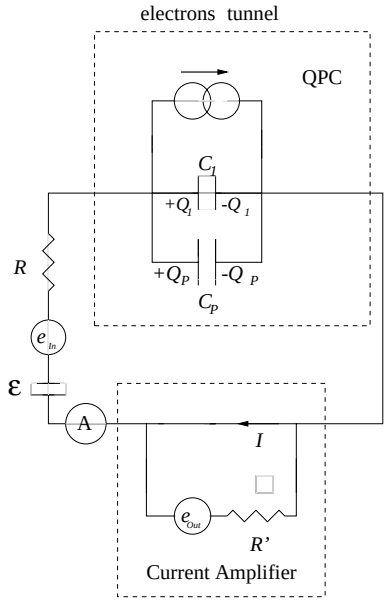

Figure 2. Equivalent circuit for measurement of current through the QPC. The QPC is modelled as a capacitor C_1. A *parasitic* capacitance, C_P, between the source and drain is included in parallel with the QPC. Tunnelling events through the QPC are modelled as a current source.

is the interaction between the two dots. We assume that the tunnelling through the QPC is one way only and the tunnelling rate is larger than all other rates, and the QPC can be adiabatically eliminated.[1] The unconditional quantum master equation for the state of the qubit is given by[1]

$$\begin{aligned} \frac{d\rho(t)}{dt} &= -i[H,\rho(t)] + \gamma\mathcal{D}[n_1]\rho(t) \\ &= \mathcal{L}\rho(t), \end{aligned} \tag{2}$$

where $\gamma = 2\lambda_0 + \lambda_1$ is the decoherence rate of the qubit, λ_0 and λ_1 are the tunnelling rates through the QPC introduced in section 2, $n_1 = c_1^\dagger c_1$ is the occupation number of dot1 and we have adopted the convention of $\hbar = 1$. The second line of equation (2) defines the Louivillian super-operator, $\mathcal{L}$. This master equation is of the Lindblad form[12] for valid evolution* derived in the appendix of reference1,[1] where

$$\mathcal{D}[X]Y \equiv XYX^\dagger - \frac{1}{2}(X^\dagger XY + YX^\dagger X), \tag{3}$$

The tunnelling increment $dN(t)$ is formally defined by:

$$dN^2 = dN \tag{4}$$

$$\begin{aligned} \mathrm{E}\left[\frac{dN(t)}{dt}\right] &= \lambda_0 \mathrm{Tr}\left[(1-n_1)\rho_c(t)(1-n_1)\right] \\ &\quad +(\lambda_0+\lambda_1)\mathrm{Tr}\left[n_1\rho_c(t)n_1\right] \\ &= \lambda_0 + \lambda_1\langle n_1\rangle_c(t) \end{aligned} \tag{5}$$

Notice that the (classical) expectation values have been expressed as quantum averages.

*That is, preserving the Hermiticity, norm and positivity of ρ.

We define the current through the QPC in terms of the discrete Poissonian process $dN(t)$:

$$i(t) = q\frac{dN(t)}{dt} \tag{6}$$

where $q = -|q|$ is the charge on an electron.

Here we present the quantum trajectory (stochastic master equation) for the case of ideal measurement. Omitting the time argument for simplicity, the Itô form of the stochastic master equation is[1]

$$\begin{aligned} d\rho_c &= dN\left[\frac{\mathbf{J}}{\mathrm{Tr}[\mathbf{J}\rho_c]} - 1\right]\rho_c \\ &\quad + dt\{-\lambda_1\mathcal{A}[n_1]\rho_c + \lambda_1\mathrm{Tr}[\rho_c n_1]\rho - i[H,\rho_c]\}. \end{aligned} \tag{7}$$

where the super-operator $\mathbf{J}$ is defined as $\mathbf{J}\rho_c = \lambda_0\rho_c + \lambda_1\mathcal{J}[n_1]\rho_c + 2\lambda_0\mathcal{D}[n_1]\rho_c$ for simplicity and $\mathcal{J}$ is defined by $\mathcal{J}[X]Y \equiv XYX^\dagger$. It is useful to note that the expectation value of $dN(t)$ is expressible in terms of $\mathbf{J}$ as

$$\mathrm{E}\left[\frac{dN(t)}{dt}\right] = \mathrm{Tr}[\mathbf{J}\rho_c(t)] \tag{8}$$

A quantum trajectory describes the stochastic evolution of the state matrix, $\rho_c(t)$. The evolution is *conditioned* on tunnelling events through the QPC at earlier times, hence the subscript c. Averaging the quantum trajectory over the observed stochastic processes (in this case by setting dN equal to its expectation value) recovers the unconditional master equation, (2).

3.2. Non-ideal QPC case

We analyze the equivalent circuit of figure 2 using Kirchhoff's laws and obtain the following Itô differential equation[11] for the charge on the parasitic capacitor, $Q(t)$:

$$dQ(t) = -\left(\alpha Q(t) + \beta + \sqrt{D_{\mathrm{In}}}\frac{dW_{\mathrm{In}}(t)}{dt}\right)dt + qdN(t) \tag{9}$$

where $dW_{\mathrm{In}}(t)$ is the input noise Wiener process ,[11] $\alpha = 1/RC$, $\beta = \varepsilon/R$ and $D_{\mathrm{In}} = 4\mathrm{k}_B T/R$. k_B is Boltzmann's constant and the circuit component values R and T are defined in figure 2; $dN(t)$ is the discrete tunnelling process defined by equations (4) and (5). The positive sign on the tunnelling increment is a result of our definition of the direction of the current in the circuit.

The solution of equation (9) is

$$\begin{aligned} Q(t) &= -\frac{\beta}{\alpha} + \sqrt{D_{\mathrm{In}}}e^{-\alpha t}\int_{-\infty}^{t} e^{\alpha t_1}\frac{dW_{\mathrm{In}}(t_1)}{dt_1}dt_1 \\ &\quad + qe^{-\alpha t}\int_{-\infty}^{t} e^{\alpha t_1}\frac{dN(t_1)}{dt_1}dt_1 \end{aligned} \tag{10}$$

Further analysis of the equivalent circuit of Fig. 2 with Kirchhoff's laws yields the following expression for the measured current

$$I(t) = -\alpha Q(t) - \beta + \sqrt{D_{\mathrm{In}}}\frac{dW_{\mathrm{In}}(t)}{dt} + \sqrt{D_{\mathrm{Out}}}\frac{dW_{\mathrm{Out}}(t)}{dt} \tag{11}$$

where $D_{\mathrm{Out}} = 4\mathrm{k}_B T'/R'$ and dW_{Out} is the output noise Wiener increment.

Substitution of equation (10) into this expression yields

$$\begin{aligned} I(t) &= -\alpha\sqrt{D_{\rm In}}e^{-\alpha t}\int_{-\infty}^{t} e^{\alpha t_1}\frac{dW_{\rm In}(t_1)}{dt_1}dt_1 - \alpha q e^{-\alpha t}\int_{-\infty}^{t} e^{\alpha t_1}\frac{dN(t_1)}{dt_1}dt_1 \\ &\quad +\sqrt{D_{\rm In}}\frac{dW_{\rm In}(t)}{dt} + \sqrt{D_{\rm Out}}\frac{dW_{\rm Out}(t)}{dt} \end{aligned} \tag{12}$$

In a realistic situation, an experimentalist has access to the current $I(t)$, not to the point process dN/dt. Thus the realistic conditional state of the system would be conditioned upon $I(t)$, rather than upon dN/dt as in Eq. 7. It is possible to do this, following the method introduced for photodetectors in Refs..[14, 15] The result is a stochastic Fokker-Planck equation for $\rho_c(Q)$, where $\mathrm{Tr}[\rho_c(Q)$ is the conditional probability that the charge on the capacitor is Q, and where $\int dQ\rho_c(Q)$ is the conditional quantum state, averaged over the unobserved charge Q. The details of this equation, and its derivation, will be left to a future publication.

4. NOISE POWER SPECTRA

Noise is characterized by its power spectrum $S(\omega)$, which is the Fourier transform of the current-current two-time autocorrelation function,[13] $G(\tau)$:

$$G(\tau) = \langle i(t)i(t+\tau)\rangle_{ss} - \langle i(t)\rangle_{ss}\langle i(t+\tau)\rangle_{ss} \tag{13}$$

where $i(t)$ represents the current through the QPC as a function of time and $\langle K\rangle_{ss}$ denotes the steady-state (quantum) average of K. The noise spectrum is expressible as[1]

$$S(\omega) = 2\int_0^\infty G(\tau)\cos(\omega\tau)d\tau \tag{14}$$

To characterize the noise involved in the detection of qubit states by a QPC, we derive the noise power spectrum. Two types of noise are considered in this study: Johnson noise due to thermal motion of electrons and shot noise due to the discreteness of the charge of electrons. In the steady state, Johnson noise is *white* noise which has a flat power spectrum. The voltage spectrum is given by[16]

$$S = 4k_BTR \tag{15}$$

where k_B is Boltzmann's constant, T is the absolute temperature of the conductor and R is the conductor resistance. This approximation of Johnson noise as white noise is actually valid for many practical situations, not just in the steady state.[16]

In devices such as p-n junctions and tunnel junctions, the transfer of electrons can be described by Poisson statistics.[13] For these devices, the shot noise has its maximum value

$$S = 2qI_m \equiv S_{Poisson} \tag{16}$$

where q is the electronic charge and I_m is the time-averaged mean current through the device. This is valid for electron pulse widths less than $1/\omega$. The shot noise can be suppressed below $S_{Poisson}$ by correlations.[13]

When plotting the noise spectrum, we use dimensionless parameters and normalize $S(\omega)$ by the full shot noise level $2qI_m$ to produce what is known as the *Fano factor*

$$F(\omega) = \frac{S(\omega)}{2qI_{ss}} \tag{17}$$

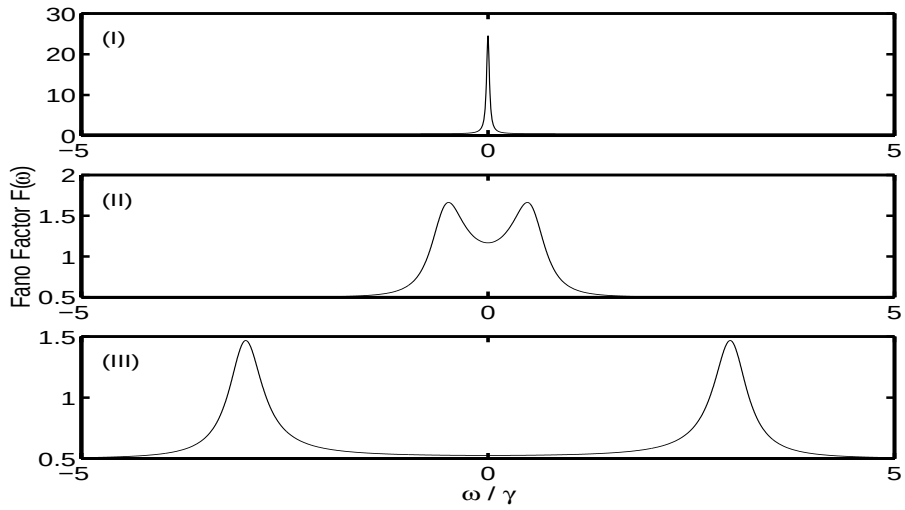

Figure 3. Fano Factor plots for ideal QPC measurement of the current for different values of the tunnel coupling between qubit dots: (I) $\Omega = 0.1\gamma$, (II) $\Omega = 0.6\gamma$, (III) $\Omega = 3\gamma$.

4.1. Noise spectrum in the Ideal QPC case

The noise in this case is purely due to the stochastic nature of the quantum processes. The processes that produce shot noise are represented by the stochastic point process $dN(t)$. The current tunnelling through the QPC in this case is derived in section 3.1. Using the definition (13) yields the following steady-state autocorrelation function:

$$G(\tau) = qi_{ss}\delta(\tau) + \frac{e^2\lambda_1^2}{8}\left(\frac{b_+e^{b_-\tau} - b_-e^{b_+\tau}}{\sqrt{(\gamma/4)^2 - \Omega^2}}\right) \tag{18}$$

where

$$b_\pm = -\gamma/4 \pm \sqrt{(\gamma/4)^2 - \Omega^2} \tag{19}$$

are two (possibly complex) numbers with non-positive real parts; $\gamma = 2\lambda_0 + \lambda_1$ is the decoherence rate of the qubit[1] and Ω is the coupling frequency between the qubit dots (both introduced in Sect. 3). The Fourier transform of $G(\tau)$ gives the noise spectrum:

$$S(\omega) = qi_{ss} + \frac{e^2\lambda_1^2\Omega^2}{4\sqrt{(\gamma/4)^2 - \Omega^2}}\left[\frac{1}{b_+^2 + \omega^2} - \frac{1}{b_-^2 + \omega^2}\right] \tag{20}$$

In order to visualize the characteristics of the noise properties of the measurement we plot the noise spectra (as a Fano Factor plot) in Fig. 3 for three different values of Ω corresponding to the cases of weak (top), intermediate (middle)and strong coupling between the two dots, respectively. The double peaked structure indicates coherent tunnelling between the qubit dots. The separation of the peaks is a measure of the strength of the tunnel coupling - larger separation corresponds to stronger coherence in tunnelling between the qubit dots.

4.2. Noise Spectrum in the Non-Ideal QPC Case

The expression for the measured current in the non-ideal circuit was derived in Sect. 3.2 as Eq. 11. We now substitute Eq. 12 into Eq. 13 to calculate the steady-state two-time autocorrelation function and obtain:

$$
\begin{aligned}
G(\tau) &= qI_{ss}\delta(\tau) + D_{\mathrm{Out}}\delta(\tau) + D_{\mathrm{In}}\left(\delta(\tau) - \frac{\alpha}{2}e^{-\alpha\tau}\right) \\
&+ \frac{\alpha^2 e^2 \lambda_1^2}{8\sqrt{(\gamma/4)^2 - \Omega^2}}\left\{\frac{b_+}{\alpha^2 - b_-^2}e^{b_-\tau} - \frac{b_-}{\alpha^2 - b_+^2}e^{b_+\tau}\right. \\
&\left. + \left(\frac{b_+}{\alpha^2 - b_-^2} - \frac{b_-}{\alpha^2 - b_+^2} + \frac{b_-}{\alpha\left(\alpha + b_+\right)} - \frac{b_+}{\alpha\left(\alpha + b_-\right)}\right)e^{-\alpha\tau}\right\}
\end{aligned}
\tag{21}
$$

The corresponding noise spectrum is evaluated using Eq. 14 and is:

$$
\begin{aligned}
S(\omega) &= qI_{ss} + D_{\mathrm{Out}} + D_{\mathrm{In}}\left(1 - \frac{\alpha^2}{\alpha^2 + \omega^2}\right) \\
&+ \frac{e^2\lambda_1^2\Omega^2}{4\sqrt{(\gamma/4)^2 - \Omega^2}}\left[\frac{1}{b_+^2 + \omega^2} - \frac{1}{b_-^2 + \omega^2}\right]\left(\frac{\alpha^2}{\alpha^2 + \omega^2}\right)
\end{aligned}
\tag{22}
$$

where $b_\pm$ is defined by equation (19) and $\alpha = 1/RC$.

The calculated results for various parameters are plotted in Figs. 4, 5 and 6. For comparison with the plots of the ideal spectrum (that is, the noise spectrum for ideal measurement), we plot the non-ideal spectrum using the same values for the tunnelling rate between the qubit dots, Ω. The influence of the non-ideal circuit components is shown in the non-ideal spectra of Figs. 4, 5 and 6 for strong, intermediate and weak coupling strength between the qubit dots, respectively.

Figure 4 shows that the non-ideal circuit components have a very strong influence on the noise spectrum features for strong tunnel coupling between the qubit dots. In the top plot, where $R = 100\ ohms$ and $C = 10\ pF$, this influence is so strong that the original spectral features that provide information about the qubit are almost unidentifiable. The sharp peaks have been suppressed by the measurement circuit into small bumps in the wings of the spectrum. These values of the parasitic variables R and C are chosen from the literature[17] as realistic values. As the parasitic capacitance is decreased (the lower two plots) in the Fig. 4, the bandwidth of the high-pass filter broadens and the 'wings' decrease to a negligible height within the domain shown - physically this corresponds to the input white noise being filtered out of the measured current. The original features of the ideal noise spectrum (III) in Fig. 3 are recovered. These results can be used to determine the value of the combination of non-ideal circuit components (RC) for which the measurement device and circuit can be well approximated by the ideal model or where information about the quantum system can no longer be obtained from the measurement.

For intermediate tunnel coupling strength between the qubit dots, figure 5 shows a weaker influence of the non-ideal circuit components on the features of the noise spectrum. The filter shape remains identical, but the peaks are not suppressed by as much as for stronger coupling (i.e. higher rates). We chose the values of the parasitic variables R and C to be the same as in figure 4 for comparison. The peaks showing the coupling strength between the qubit dots are easily visible in all three plots, i.e. for all three values of RC. This suggests that, for intermediate coupling strength between the qubit dots, information about the qubit is more readily obtainable by non-ideal measurement (provided $RC < 10^{-9}s$) than for stronger coupling strength.

For weak coupling between the qubit dots, as shown in figure 6, the non-ideal circuit components have a negligible influence on the noise spectrum features. The spectra are very close to the spectrum in the ideal QPC case, (I) in Fig. 3.

In summary, we have found that the non-ideal circuit components increased the current noise. The influence of the (classical) non-ideal circuit components on the features of the noise spectrum that provide information about the quantum system (qubit) is greatest for strong tunnelling coherence between the qubit dots. That is,

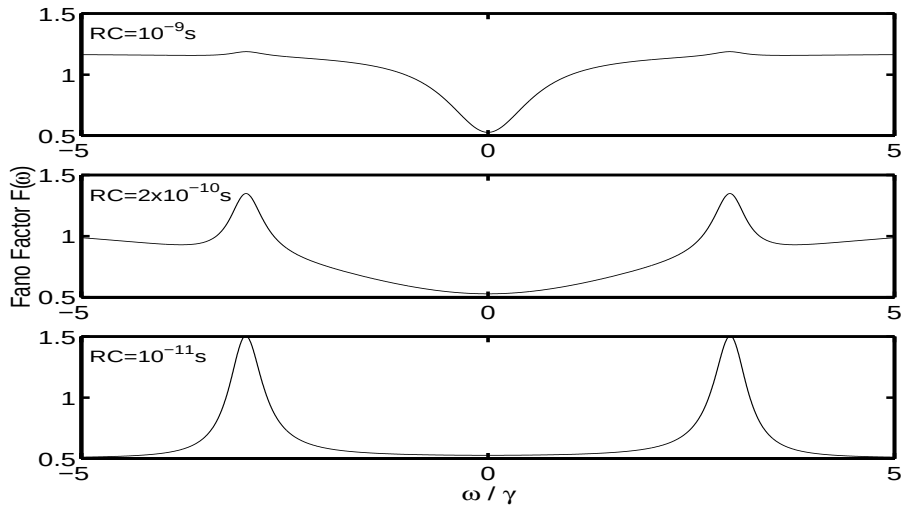

Figure 4. Fano Factor plot for non-ideal QPC measurement of the current when the coupling between the qubit dots is relatively strong: $\Omega = 3\gamma$.

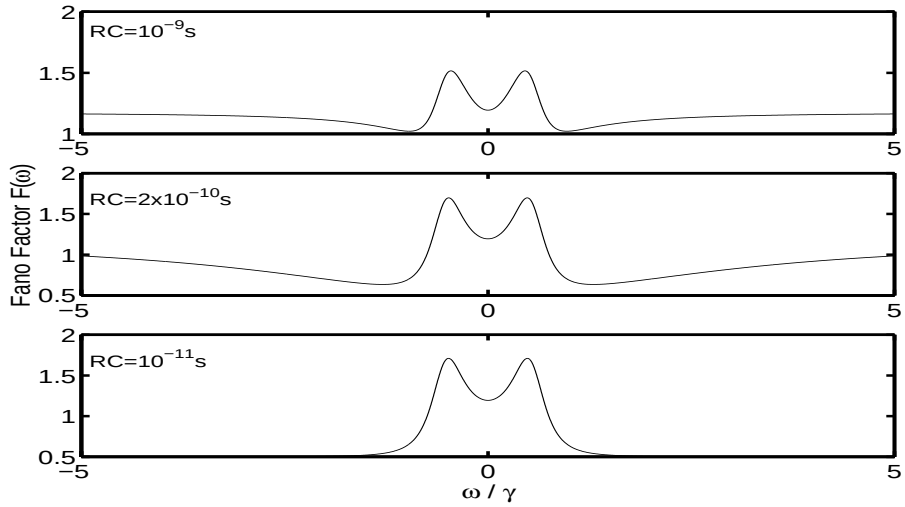

Figure 5. Fano Factor plot for non-ideal QPC measurement of the current when the coupling rate between the qubit dots is an intermediate value: $\Omega = 0.6\gamma$.

for strong coupling between the qubit dots, it is difficult to obtain information about the qubit in a non-ideal measurement (for the realistic value of $RC \approx 10^{-9}s$). The non-ideal noise spectrum can also be used to determine limits of applicability of the non-ideal and ideal models. That is, we can estimate values of the combination of non-ideal circuit components R and C for which the non-ideal model can be approximated by the ideal model.

5. SUMMARY

We extend our quantum stochastic approach to the measurement of the states of the coupled quantum dot system using a non-ideal QPC. We use an equivalent circuit to model the realistic devices. The current through the detector QPC is derived using a quantum trajectory. We then calculated the current noise power spectrum and

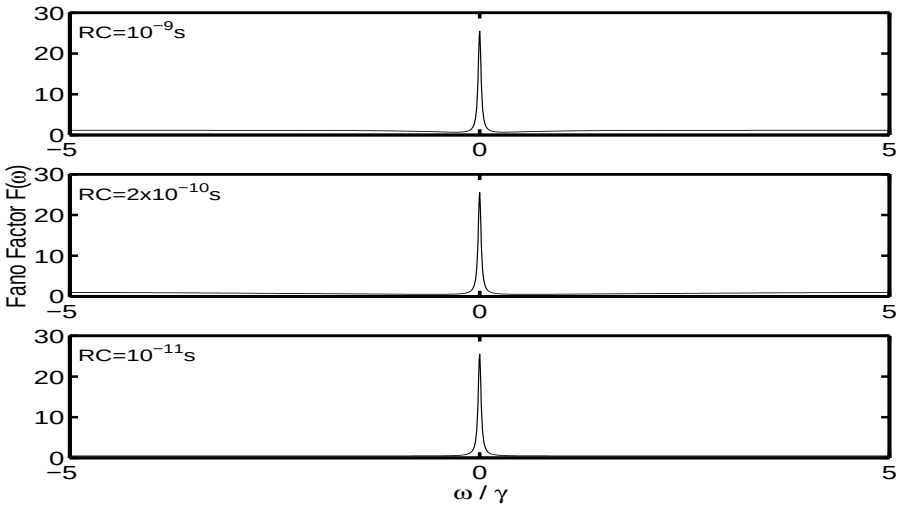

Figure 6. Fano Factor plot for non-ideal QPC measurement of the current when the coupling between the qubit dots is weak: $\Omega = 0.1\gamma$.

found that, in general, the non-ideal circuit components increased the current noise. We showed that the influence of the non-ideal circuit components on the current noise spectrum is greatest for strong tunnelling coherence between the qubit dots. We also found that, for this strong coupling, it is difficult to obtain information about the quantum processes within the qubit from non-ideal measurement. The non-ideal spectrum can also be used to make estimates pertaining to the limits of applicability of the non-ideal and ideal models.

REFERENCES

1. H.M. Wiseman, Dian Wahyu Utami, He Bi Sun, G.J. Milburn, B.E. Kane, A. Dzurak and R.G. Clark, "Quantum measurement of coherent tunneling between quantum dots," *Physical Review B* **63**, 235308, 2001.
2. G. Schön, A. Schnirman and Y. Makhlin "Josephson-junction qubits and the readout process by single-electron transistors", */cond-mat/*9811029, 1998.
3. Alexander N. Korotkov, "Continuous quantum measurement of a double dot," *Phys. Rev. B* **60**, 5737, 1999.
4. B.E. Kane, "A silicon-based nuclear spin quantum computer", *Nature* **393**, 133, 1998.
5. D. Loss, D.P. DiVincenzo, "Quantum computation with quantum dots", *Phys. Rev. A* **57**, 120, 1998.
6. A. Shnirman, G. Schön and Z. Hermon, "Quantum manipulations of small Josephson junctions", *Phys. Rev. Lett.* **79**, 2371, 1997.
7. S.A. Gurvitz, "Measurements with a noninvasive detector and dephasing mechanism," *Phys. Rev. B* **56** 15215, 1997.
8. Hsi-Sheng Goan, G.J. Milburn, H.M. Wiseman and He Bi Sun, "Continuous measurement of two coupled quantum dots using a point contact: A quantum trajectory approach," *Phys. Rev. B* **63** 125326, 2001.
9. M.H. Devoret and R.J. Schoelkopf, "Amplifying quantum signals with the single-electron transistor," *Nature* **406**, 1039 2000.
10. T. Ando et al., *Mesoscopic physics and electronics*, Springer, New York, 1998.
11. C.W. Gardiner, *Handbook of Stochastic Methods for the Physical and Chemical Sciences*, Springer, Berlin, 1985. (2001).
12. G. Lindblad:, "On Generators of Quantum Dynamical Semigroups," *Commun. Math. Phys.* **48**, 199, 1976.

13. M.J.M. de Jong and C.W.J. Beenakker: "Shot noise in mesoscopic systems," in *Mesoscopic Electron Transport*, L.L. Sohn, L.P. Kouwenhoven and G. Schön, ed., NATO ASI Series E345, pp. 225-258, Kluwer, Dordrecht, 1997.
14. P. Warszawski, H.M. Wiseman, and H. Mabuchi, "Quantum Trajectories for Realistic Photodetection", *Phys. Rev. A* **65**, 023802 2002.
15. P. Warszawski and H.M. Wiseman, "Quantum Trajectories for Realistic Photodetection I: General Formalism," *J. Opt. B* **5**, 1, 2003; "Quantum Trajectories for Realistic Photodetection II: Application and Analysis," *ibid.*, **5**, 15, 2003.
16. G.J. Milburn and He Bi Sun, "Classical and quantum noise in electronic systems", *Contemporary Physics*, **39**, number 1, pp. 67-79, 1998.
17. M.H. Devoret and H. Grabert, "Introduction to single charge tunneling", in *Single Charge Tunneling*, H. Grabert and M.H. Devoret, ed. NATO ASI Series, pp. 1-19, Plenum Press, New York, 1991.